

SufE D74R Substitution Alters Active Site Loop Dynamics To Further Enhance SufE Interaction with the SufS Cysteine Desulfurase

Yuyuan Dai,^{†,§} Dokyong Kim,[‡] Guangchao Dong,[†] Laura S. Busenlehner,[‡] Patrick A. Frantom,^{*,‡} and F. Wayne Outten^{*,†}

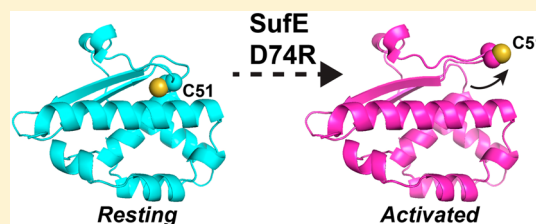
[†]Department of Chemistry and Biochemistry, University of South Carolina, Columbia, South Carolina 29208, United States

[‡]Department of Chemistry, The University of Alabama, Tuscaloosa, Alabama 35487, United States

S Supporting Information

ABSTRACT: Many essential metalloproteins require iron–sulfur (Fe–S) cluster cofactors for their function. In vivo persulfide formation from L-cysteine is a key step in the biogenesis of Fe–S clusters in most organisms. In *Escherichia coli*, the SufS cysteine desulfurase mobilizes persulfide from L-cysteine via a PLP-dependent ping-pong reaction. SufS requires the SufE partner protein to transfer the persulfide to the SufB Fe–S cluster scaffold. Without SufE, the SufS enzyme fails to efficiently turn over and remains locked in the persulfide-bound state. Coordinated protein–protein interactions mediate sulfur transfer from SufS to SufE.

Multiple studies have suggested that SufE must undergo a conformational change to extend its active site Cys loop during sulfur transfer from SufS. To test this putative model, we mutated SufE Asp74 to Arg (D74R) to increase the dynamics of the SufE Cys51 loop. Amide hydrogen/deuterium exchange mass spectrometry (HDX-MS) analysis of SufE D74R revealed an increase in solvent accessibility and dynamics in the loop containing the active site Cys51 used to accept persulfide from SufS. Our results indicate that the mutant protein has a stronger binding affinity for SufS than that of wild-type SufE. In addition, SufE D74R can still enhance SufS desulfurase activity and did not show saturation at higher SufE D74R concentrations, unlike wild-type SufE. These results show that dynamic changes may shift SufE to a sulfur-acceptor state that interacts more strongly with SufS.



Iron–sulfur (Fe–S) clusters are a widely used inorganic cofactor used for many essential cellular pathways, including respiration, amino acid biosynthesis, and central carbon metabolism. Due to the inherent toxicity of iron and sulfide, a complex series of protein–protein interactions is required for Fe–S cluster biogenesis in vivo. The first steps of Fe–S cluster biogenesis result in the formation of an Fe–S cluster on a scaffold protein. The scaffold protein then transfers the intact cluster into a pool of Fe–S cluster trafficking proteins that moves clusters to their final target metalloproteins. In the model organism *Escherichia coli*, the cysteine desulfurase SufS and its partner protein SufE work together to mobilize persulfide from L-cysteine, which is then donated to the SufB Fe–S scaffold protein.^{1–3} SufS first removes sulfur from the side chain of substrate L-cysteine to form a protein-bound persulfide species at Cys364.^{4–7} Next, SufE Cys51 functions as the second substrate in a ping-pong mechanism, where it removes the persulfide from SufS via a nucleophilic attack.^{1,2,8,9} Thus, SufE is required for complete turn over and full activity of SufS. Previously, it has been shown that *E. coli* SufS interacts with SufE even in the absence of L-cysteine substrate and that SufE may play a more active role in promoting the first step of the ping-pong reaction (removal of sulfur from L-cysteine).^{1–3,10}

SufS is a pyridoxal 5'-phosphate (PLP)-dependent dimeric enzyme and belongs to the group II desulfurase enzyme family, the members of which share similar structures and have low

basal activity.^{4,6} SufS homologues have several structural features that distinguish them from group I desulfurases like IscS or NifS.^{5,7,11} A key structural difference between SufS and the group I desulfurases like IscS is that the extended lobe of SufS containing the active site loop has an 11-residue deletion compared with that of IscS. The shortening of this region in SufS structurally restricts the flexibility of the SufS Cys364-anchoring extended lobe. The decreased flexibility results in a more ordered structure such that the active site cysteine Cys364 in SufS is clearly visible on a loop of the extended lobe (Thr362–Arg375 for *E. coli* SufS).^{5,7,11} In contrast, the corresponding loop (Ala327–Leu333) of IscS is longer and disordered in most structures of IscS due to its flexibility.^{12–14}

Group II cysteine desulfurases characterized to date require a specific sulfur shuttle protein for full activity. For *E. coli* SufS, it is SufE.^{1,2} SufE is predominantly monomeric in solution, and its structure shows that active site Cys51 occurs at the tip of a loop where its side chain is buried from solvent exposure in a hydrophobic cavity.^{15–17} The orientation of SufS and SufE active site Cys loops likely protects those proteins from oxidation during exposure to H₂O₂.⁸ However, SufS Cys364 and SufE Cys51 must come into close proximity to facilitate persulfide transfer. While the dynamics of SufS–SufE

Received: June 15, 2015

Revised: July 14, 2015

Published: July 14, 2015



interactions have been intensively studied, the structure of the SufS–SufE complex and the molecular details of how SufS and SufE interact are not clear.^{1–3,8–10}

Recently, a costructure of two homologous proteins, cysteine desulfurase CsdA (YgdJ) and its partner protein CsdE (YgdK), was solved.¹⁸ CsdE shares 35% sequence identity with SufE, and CsdA shares 45% sequence identity with SufS. The overall structure of SufE and CsdE monomers in the resting state is very similar.^{15,16} When CsdE interacts with its partner protein CsdA, the CsdE active site Cys loop (containing Cys61) is flipped out of its hydrophobic groove and moves approximately 11 Å.¹⁸ This movement is thought to facilitate interaction between the CsdA active site Cys and Cys61 of CsdE. Using hydrogen–deuterium exchange mass spectrometry (HDX-MS), we observed similar increases in the solvent accessibility of the SufE Cys51 loop upon interaction with SufS.¹⁰ Together, these results indicate that the active conformation of SufE and its homologues is one where the active site Cys loop is flipped out of its hydrophobic groove into a more extended conformation.

Examination of the structure of resting SufE shows a variety of interactions that hold the active site loop folded down into the interior of SufE.^{15,17} However, that loop is under torsional strain due to a somewhat unusual *cis* peptide bond involving Cys51 and the positioning of Gly50 to facilitate conformational changes that relieve the stress. We reasoned that subtle point mutations that disrupt some of the stabilizing interactions may activate the Cys51 loop by allowing it to flip out of the hydrophobic groove. In this study, we characterized one such mutation, conversion of Asp74 to Arg, and demonstrated its effects on SufE structure as well as SufS–SufE interactions. We found that the SufE D74R substitution actually increased SufE interaction with SufS and showed unusual enhancement of SufS activity. These results suggest that the SufE D74R substitution leads to structural changes in the SufE protein that flip the loop containing active site Cys51 into a sulfur-accepting conformation, which increases the interaction of SufE with SufS and its ability to mobilize SufS persulfide.

■ EXPERIMENTAL PROCEDURES

Strains, Plasmids, and Growth Conditions. For mutagenesis of *sufE*, pET21a_*sufE* was used as a template.⁸ The SufE D74R substitution was introduced by site-directed mutagenesis using the QuikChange kit (Stratagene) with primers 5′-AGGGCGACAGCCGTGCGGCGATTGT-3′ and its complementary primer 5′-ACAATCGCCGCACGGC-TGTCGCCCT-3′ on pET21a_*sufE*. The SufE (C17S-D74R) double mutation was introduced by site-directed mutagenesis using the QuikChange Kit (Stratagene) with primers 5′-TTTTACGCTCCGCCAACTGGGAAGA-3′ and its complementary primer 5′-TCTTCCCAGTTGGCGGAGCGTAAAA-3′ on pET21a_*SufE* D74R.

Protein Expression and Purification. *E. coli* SufS and SufE were independently expressed and purified as described previously.⁸ *E. coli* BL21(DE3) containing the pET-21a_*SufE* D74R plasmid was grown in LB with 100 µg/mL ampicillin at 37 °C overnight, diluted 100-fold into LB, and induced by 500 µM isopropyl-1-thio-β-D-galactopyranoside (IPTG) when the cultures reached an OD₆₀₀ of 0.4–0.6. Induction was at 18 °C overnight. Cells were harvested and lysed in 25 mM Tris, pH 7.5, 100 mM NaCl, 5 mM DTT, and 1 mM phenylmethylsulfonyl fluoride via sonication. Following centrifugation at 20 000g for 30 min, lysate was filtered before loading on columns. SufE D74R was purified using Q-sepharose and

Superdex 75 chromatography resins in sequence. The Q-sepharose column utilized a linear gradient from 25 mM Tris-HCl, pH 7.5, 10 mM βME to 25 mM Tris-HCl, pH 7.5, 1 M NaCl, 10 mM βME. The Superdex column was run with 25 mM Tris-HCl, pH 7.5, 150 mM NaCl, and 5 mM DTT. Purified proteins were concentrated, frozen as drops in liquid nitrogen, and stored at –80 °C until further use.

Cysteine Desulfurase Activity Assays. Cysteine desulfurase activity was measured with *N,N*-dimethyl-*p*-phenylenediamine sulfate (NNDP) and FeCl₃ using a slightly modified published protocol.² Reactions were carried out aerobically in 25 mM Tris-HCl, pH 7.4, 150 mM NaCl at 27 °C. Proteins were incubated with 2 mM DTT for 5 min prior to addition of L-cysteine in a total reaction volume of 800 µL. Reactions were allowed to proceed for 10 min and then were stopped by the addition of 100 µL 20 mM NNDP in 7.2 M HCl and 100 µL of 30 mM FeCl₃ in 1.2 M HCl. The mixture was incubated for 30 min in the dark to form methylene blue. Precipitated protein was removed by 1 min centrifugation at 16 100g, and the methylene blue was measured at 670 nm. A Na₂S standard solution was used for calibration.

Circular Dichroism Spectroscopic Analysis. Circular dichroism (CD) spectra were measured using a JASCO J815 spectropolarimeter (JASCO, Essex, UK) at 20 °C. SufE or SufE D74R was prepared at 20 µM concentration in 25 mM, pH 8.0, boric acid buffer. Far-ultraviolet (180–300 nm) spectra were collected with a cuvette of 1 cm path length.

Cysteine Binding Assays. All assays were performed at room temperature in 25 mM Tris-HCl, 150 mM NaCl, pH 7.4. L-Cysteine binding was evaluated as described previously by monitoring the immediate ΔA₄₂₀ or ΔA₃₄₀ elicited by the addition of increasing concentrations of L-cysteine to 25 µM SufS_{apo} or 25 µM SufS_{apo} with an equal amount of SufE D74R_{alk}.¹⁰ Protein was first added to the cuvettes followed by L-cysteine and mixed for ~5 s prior to a wavelength scan from 200 to 650 nm. As L-cysteine concentrations increased (0, 12.5, 25, 30, 37.5, 50, 75, 100, 250, 500, 750, and 1000 µM), the 420 nm PLP peak intensity (internal aldimine) decreased and a new 340 nm peak (external aldimine) increased in intensity. Data were analyzed with Prism software (GraphPad). SufS_{apo}–SufE D74R_{alk}–Cys data was best fit with a one-site-specific binding with Hill slope model. SufE D74R_{alk} was prepared by first preincubating with 5 mM DTT for 30 min followed by removal of DTT with a 5 mL desalting column. SufE was then incubated with 5 mM iodoacetamide for 1 h in the dark and was exchanged into desulfurase assay buffer with a desalting column.

Isothermal Titration Calorimetry (ITC). ITC measurements were performed on a VP-ITC calorimeter (MicroCal) at 27 °C. For the SufS_{apo} and SufE D74R_{apo} ITC experiment, SufS_{apo} present in the cell (1.44 mL at 50 µM) was titrated with 45 × 6 µL injections of 1.1 mM SufE (a 10-fold molar excess over SufS_{apo}). The duration of each injection was 7.2 s (1.2 s/µL), with an interval of 200 s between injections. Each experiment was corrected for the endothermic heat of injection resulting from the titration of SufE D74R into buffer. SufS_{apo}–SufE_{apo} ITC data were analyzed with the two sequential binding sites model in MicroCal Origin using a SufS_{apo} dimer concentration of 54 µM. SufS_{apo}–SufE D74R ITC data was analyzed with the one-site model in MicroCal Origin using a SufS monomer concentration of 500 µM.

PDT-Bimane for pK_a Measurement of Cysteine Residue C51 on SufE. For pK_a measurement of Cys51 in

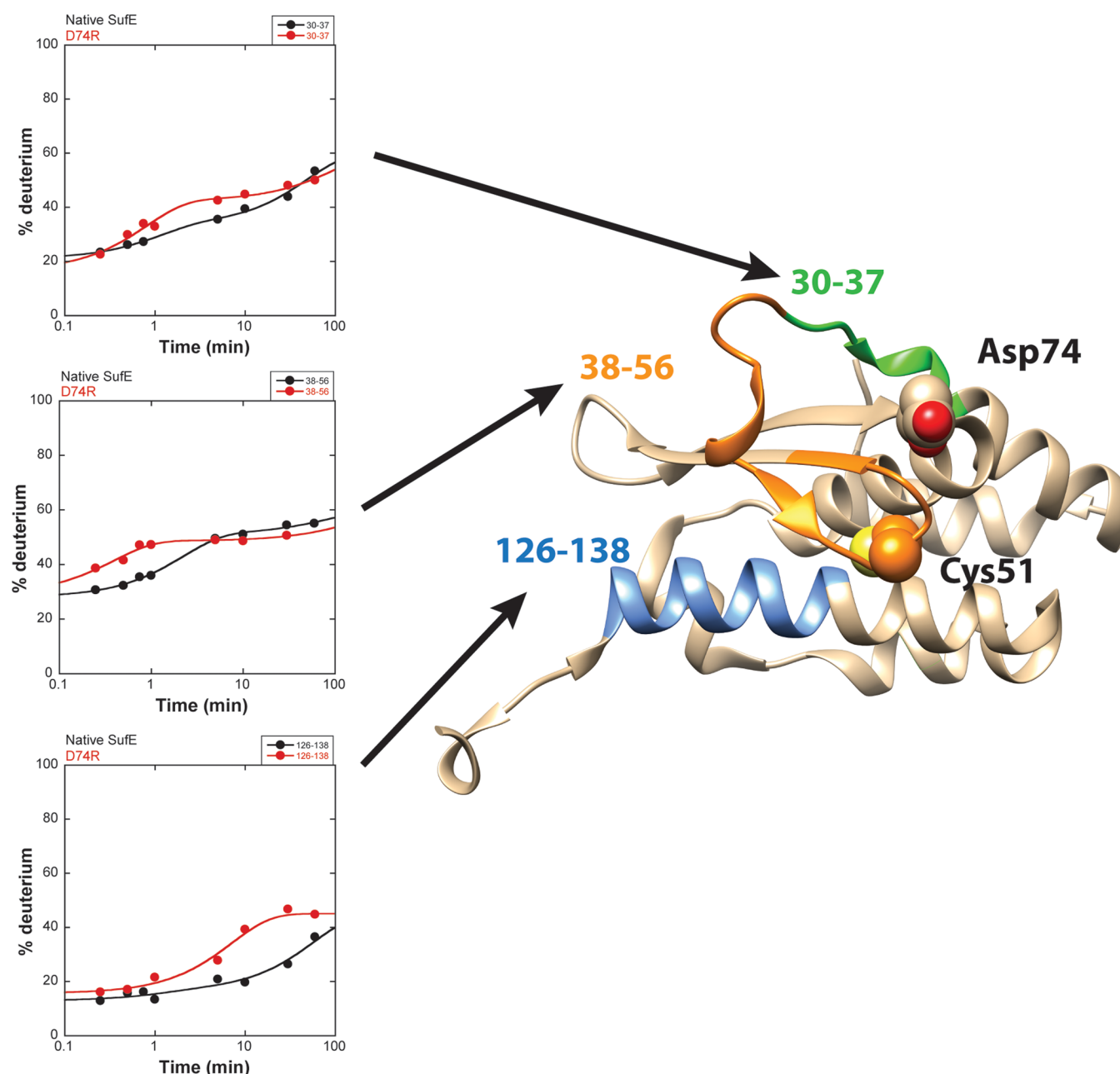


Figure 1. HDX-MS kinetic traces comparing deuterium incorporation as a function of time for SufE and the SufE D74R variant. Peptides 30–37, 38–56, and 126–138 exhibit increased rates of deuterium incorporation in the D74R variant. These peptides are mapped onto the structure of SufE (PDB 1MZG), with Asp74 and Cys51 shown as spheres. Fitting parameters can be found in [Supporting Information Table S1](#). The uptake plots for all peptides are found in [Supporting Information Figure S2](#).

the SufE D74R variant, SufE C17S and SufE C17S-D74R were incubated with 50 mM DTT for 1 h at room temperature. The buffer was then exchanged to 25 mM potassium phosphate, pH 6.0, 50 mM NaCl, and 1 mM EDTA. Protein was then diluted to 10 μ M concentration in sodium citrate or phosphate buffers spanning the pH range 4–11. The reaction volume was 150 μ L, and the final PDT-Bimane concentration was 80 μ M. After rapid mixing, the absorbance at 343 nm was monitored over 120 min in a 96-well microplate. Each curve was fit to either a first- or second-order exponential function Henderson–Hasselbalch equation, $Y = Y_0 + A \exp(-X/t_1)$, and the rate constants were determined. The inverse of the rate constants (t_1) was plotted as a function of pH.

Hydrogen–Deuterium Exchange Mass Spectrometry (HDX-MS). All samples for HDX were prepared individually and run on the same day. HDX-MS was performed with 125 μ M SufE D74R in 25 mM Tris-HCl, pH 7.4, 150 mM NaCl, 10 mM 2-mercaptoethanol essentially as described previously.¹⁰ HDX samples containing 2 μ L of 125 μ M SufE D74R (5 μ M final concentration) and 23 μ L of 99.9% D₂O (80% final percent deuterium) were incubated at 25 °C for 15 s to 1 h. The reaction was quenched by adding 25 μ L of ice-cold quench buffer (0.1 M KH₂PO₄, pH 2.3 at 0 °C) and digested on ice for 5 min using 2 μ L of 5 mg/mL pepsin (porcine pepsin 3200–4500 U/mg). To analyze the SufS–SufE D74R complex, the preformed 1:1 SufS_{apo}–SufE D74R complex was generated by incubating equal volumes of 250 μ M SufS_{apo} and 250 μ M SufE

D74R for 10 min. The HDX reaction was initiated with 23 μL of 99.5% D_2O to 2 μL of the 250 μM complex (125 μM SufS_{apo} and 125 μM SufE D74R). The samples were incubated at 25 $^\circ\text{C}$ from 15 s to 1 h. The appropriate HDX control samples corresponding to the natural isotope distribution pattern for various peptides ($m_{0\%}$) and the amount of deuterium back-exchange from fully deuterated peptides ($m_{100\%}$) were also performed as described.¹⁰ The peptides were separated on a Phenomenex microbore 2 \times 50 mm C18 reverse-phase column using an Agilent 1100 HPLC inline to a Bruker HCTUltra PTM Discovery mass spectrometer in positive ion mode. A 0–50% gradient of acetonitrile over 15 min at 0.1 mL/min was used. The MS spectra from each HDX-MS sample were analyzed using HDEaminer (Sierra Analytics). Each experiment was repeated in triplicate and averaged. The percentage of deuterium incorporated for each peptide was plotted as a function of log time using KaleidaGraph (Synergy Software), and the resulting plot was fit to the sum of first-order rate expressions.¹⁹

RESULTS

The Cys51-Containing Peptide Is More Flexible in SufE D74R. To ensure that the D74R mutation does not destabilize the overall secondary or tertiary structure of the protein, we compared the circular dichroism (CD) spectra of SufE D74R and wild-type SufE in the far-UV region (190–260 nm) (Supporting Information Figure S1). Similar CD spectra were obtained for both proteins, indicating that the D74R substitution did not cause significant changes to the SufE secondary structure, which contains a mixture of α -helix and β -sheet elements (Supporting Information Figure S1A). The apparent molecular weight of SufE D74R also was monitored by gel filtration chromatography. SufE D74R elutes as a single symmetric peak at the same position as wild-type SufE, giving an apparent molecular weight of 21 323 Da, compared to an apparent molecular weight of 21 304 Da for wild-type SufE (data not shown). The theoretical MWs of SufE D74R and wild-type SufE are 15 841 Da and 15 800 Da, respectively. On the basis of this analysis, SufE D74R exists as a monomer in solution like wild-type SufE.^{1,2} The CD and gel filtration data indicate that SufE D74R is correctly folded in an overall conformation similar to wild-type SufE. The heterologous expression of the SufE D74R protein also rescues the growth defect of an *E. coli* strain lacking the *sufE* gene (ΔsufE) under oxidative stress conditions (Supporting Information Figure S1B). In this assay, SufE D74R rescued the growth defect as well as heterologous expression of wild-type SufE (Supporting Information Figure S1B). Thus, the D74R mutation does not disrupt SufE function in vivo.

HDX-MS was used to directly measure the solvent exposure of Cys51 in the SufE D74R variant (Figure 1). No significant changes were observed in the backbone conformation around the D74R substitution (peptides 66–83, 69–83, 69–84, 70–83), although there was a small increase in dynamics (Supporting Information Figure S2). The previously determined three-dimensional structure of SufE is consistent with this result, as Asp74 is in a small surface loop.^{15,16} However, an increase in solvent accessibility and dynamics was observed in the loop of residues 38–56 that contains active site Cys51 (Figure 1). This result is similar to that obtained previously for SufE where the active site Cys51 is alkylated with iodoacetamide (SufE_{alk}), but the HDX pattern is somewhat

different, suggesting the conformations are similar but not identical.¹⁰

Two additional regions show changes in backbone dynamics of SufE D74R relative to the wild-type protein. A C-terminal region containing residues 126–138 exhibits an increase in long time scale dynamics (breathing motions) (Figure 1). This region is in a helix near where the Cys51 side chain packs. Disruption of interactions between Cys51 and the helix in the D74R variant could cause this helix to lose constraints and allow for more breathing motions. There is also a slight increase in dynamics for the peptide covering residues 27–37. An overlapping peptide (residues 25–29) shows no changes in deuterium incorporation, suggesting that the actual change occurs over the region of residues 30–37 (Figure 1). This loop is adjacent to the peptide containing Cys51 (38–56) and thus could also be perturbed by a loss of interaction with the Cys51-containing loop. The HDX-MS analysis indicates that the active site loop containing Cys51 is more dynamic and solvent-exposed in the SufE D74R mutant protein.

SufE D74R Is a Better Sulfur Acceptor for SufS than Wild-Type SufE. To analyze whether SufE D74R enhances SufS activity like wild-type SufE, SufS activity was measured in the presence of different concentrations of SufE D74R and L-cysteine (Figure 2). For both wild-type and mutant SufE

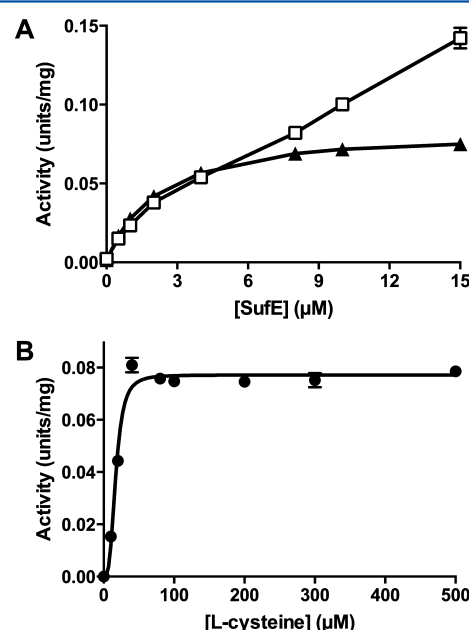


Figure 2. Kinetic analysis of SufS activity in response to varied substrate concentrations. (A) The reactions contained 0.5 μM SufS, 0–15 μM wild-type SufE (\blacktriangle) or SufE D74R (\square), 2 mM DTT, and 2 mM L-cysteine. (B) The reactions contained 0.5 μM SufS, 4 μM SufE D74R, 2 mM DTT, and 10–500 μM L-cysteine. The black line is a fit of the data with an allosteric sigmoidal model using GraphPad Prism. The fitting parameters for fits with the allosteric sigmoidal model and the Michaelis–Menten equation are shown in Supporting Information Table S2.

proteins, as SufE concentration increased, the SufS desulfurase activity increased. However, when the SufE D74R concentration increased beyond 8 μM (or a SufE/SufS molar ratio of 16:1 in this assay), SufS desulfurase activity did not saturate, as was observed for wild-type SufE, and continued to increase (Figure 2A). The failure to produce a hyperbolic activity plot indicates that SufS does not follow Michaelis–Menten behavior

in the presence of SufE D74R. To test if SufE D74R alters the kinetics of SufS for L-cysteine substrate, SufS activity was measured as a function of L-cysteine concentration with a constant SufE D74R concentration that provides a SufE/SufS ratio of 8:1 (0.5 μ M SufS with 4 μ M SufE D74R) (Figure 2B). At this ratio of SufE D74R/SufS, the maximum activity enhancement of SufS is similar to the maximum enhancement provided by wild-type SufE (Figure 2A). When the SufS enzyme kinetics were fit with the Michaelis–Menten equation, a moderate goodness of fitting was obtained ($R^2 = 0.89$) (Supporting Information Table S2). Using this fit, the K_m of SufS for L-cysteine in the presence of SufE D74R is 16.5 μ M, which is nearly 3-fold lower than the K_m obtained in the presence of an equal concentration of wild-type SufE (K_m of 43.5 μ M). Fitting the data to an allosteric sigmoidal model (black line in Figure 2B) provided a better R^2 value and showed a Hill coefficient (h) of 3.2, suggesting positive cooperativity. However, this fit had a much larger standard error for K_m (K') than the Michaelis–Menten fit (Supporting Information Table S2). On the basis of this analysis, we concluded that the SufE D74R mutation decreases the SufS K_m for L-cysteine but also deviates from Michaelis–Menten behavior at high concentrations (above SufE/SufS ratios of 16:1), where the SufS activity enhancement does not saturate, in contrast to what is observed with wild-type SufE.

SufE D74R_{alk} Alters L-Cysteine Binding to SufS to a Lesser Extent than SufE_{alk}. When L-cysteine substrate binds to SufS PLP, it displaces the internal aldimine between PLP and SufS Lys226 and forms an external aldimine at the same position with the α -amino group of the L-cysteine substrate (Supporting Information Scheme S1).^{5,7} Previously, we discovered that SufE_{apo} binding to SufS_{apo} leads to conformational changes within the SufS peptide containing Lys226 that forms the internal aldimine with PLP.¹⁰ In addition, SufE_{alk} binding to SufS altered the reactivity of PLP for L-cysteine substrate, promoting the formation of the external aldimine species.¹⁰ Alkylation of SufE Cys51 prevents sulfur transfer from SufS to SufE (i.e., SufS turnover) and allowed us to exclusively examine the effect of SufE on the first step of the reaction, L-cysteine binding to SufS PLP. To test if the D74R substitution alters the effect of SufE on the SufS PLP environment, we generated SufE D74R_{alk}. The initial binding of L-cysteine substrate to resting SufS_{apo} was compared to the SufS_{apo}–SufE D74R_{alk} complex by following the appearance of the L-cysteine external aldimine, which absorbs at 340 nm, and the disappearance of the internal aldimine, which absorbs at 420 nm (Figure 3A). Fitting the ΔA_{340} measurements to a one-site binding model with Hill slope shows that the K_d of SufS for L-cysteine is 39 μ M if one equivalent of SufE D74R_{alk} is present (Figure 3B). This value is properly thought of as an apparent dissociation constant since the assay does not distinguish between L-cysteine binding to SufS and the rate of external aldimine formation once L-cysteine is bound. Either step or both steps might be altered by SufE D74R_{alk}. This apparent K_d of 39 μ M with SufE D74R_{alk} is intermediate between the 61 ± 1.5 μ M measured for SufS alone and the 18 ± 1.6 μ M measured for SufS with one equivalent of wild-type SufE_{alk}.¹⁰ The results indicate that while the binding of SufE D74R_{alk} likely remodels the SufS_{apo} active site around PLP, the effect is less pronounced than that observed with wild-type SufE_{alk}.

D74R Substitution Slightly Reduces the Lower pK_a of Active Site Cys51 in SufE. Next, we tested if the SufE D74R substitution directly alters the pK_a of the active site Cys51

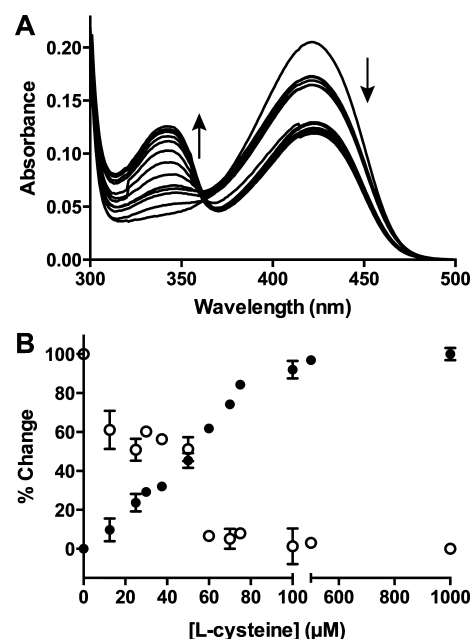


Figure 3. Spectroscopic analysis of L-cysteine binding to SufS. (A) UV–visible absorption spectra of PLP from 25 μ M SufS with 25 μ M SufE D74R_{alk} after addition of 0, 12.5, 25, 30, 37.5, 50, 75, 100, 250, 500, 750, and 1000 μ M L-cysteine. Arrows show the direction of spectral changes as L-cysteine concentrations are increased. (B) Percent change in SufS PLP internal aldimine (ΔA_{420} , open circles) and SufS PLP external aldimine with L-cysteine (ΔA_{340} , closed circles) upon addition of increasing concentrations of L-cysteine to a mixture of 25 μ M SufS and SufE D74R_{alk} (data from panel A).

sulfhydryl group. SufE has one other Cys residue at position 17, and to prevent Cys17 from interfering with the pK_a measurement, we first generated the SufE C17S and SufE C17S/D74R variants. The SufE C17S mutation did not affect SufE enhancement of SufS when generated in wild-type SufE or SufE D74R (Supporting Information Figure S3A and data not shown). The pK_a of Cys51 in SufE C17S/D74R is 5.7, which is 0.6 pH units lower than Cys51 in SufE C17S ($pK_a = 6.3$) (Supporting Information Figure S3B).²⁰ At the pH of 7.4 used in the desulfurase assay, Cys51 in SufE D74R is more prone to exist as a thiolate anion. Increased deprotonation of SufE Cys51 should facilitate the nucleophilic attack of the thiolate anion of Cys51 on the SufS Cys364 persulfide during the sulfur exchange process. At pH 7.4, the percent of Cys51 thiol deprotonated to the thiolate anion for SufE D74R is approximately 98.0%, compared to a similar 92.6% thiolate anion for wild-type SufE. The lower pK_a of Cys51 in SufE D74R could also make it easier for DTT to cleave the Cys51 persulfide in the desulfurase assay, thereby allowing the SufE D74R variant to turn over faster than wild-type SufE after it has taken the persulfide from SufS. The rate of release of persulfide from SufE Cys51 has profound effects on the overall reaction rate during the *in vitro* SufS–SufE sulfurtransferase reaction.⁹ Faster turnover of the SufE Cys51 persulfide could indirectly lead to greater enhancement of SufS activity. To test if this hypothesis explains the increased enhancement of SufS by SufE D74R, we repeated the activity assay with a constant level of the mutant or wild-type SufE and L-cysteine but while varying the DTT concentration (Supporting Information Figure S3C). We observed that the SufS enhancement by SufE D74R and wild-type SufE both increase in response to increasing DTT and that

the curves increase at similar rates. If one were to adjust the DTT response profiles to negate the inherently higher SufE D74R enhancement, then the effect of DTT would essentially be the same on both mutant and wild-type SufE proteins. This result suggests that the lower pK_a of Cys51 in SufE D74R does not make the Cys51 persulfide on mutant SufE any more sensitive to reduction by DTT than the Cys51 in wild-type SufE.

SufE D74R Binding to SufS Is Altered and Enhanced Compared to Wild-Type SufE. Since the SufE D74R substitution causes an unusual SufS activity enhancement at high levels of SufE D74R (Figure 2A), we used isothermal titration calorimetry (ITC) to directly measure SufS_{apo}–SufE D74R_{apo} binding (Figure 4). In this context, the term apo refers

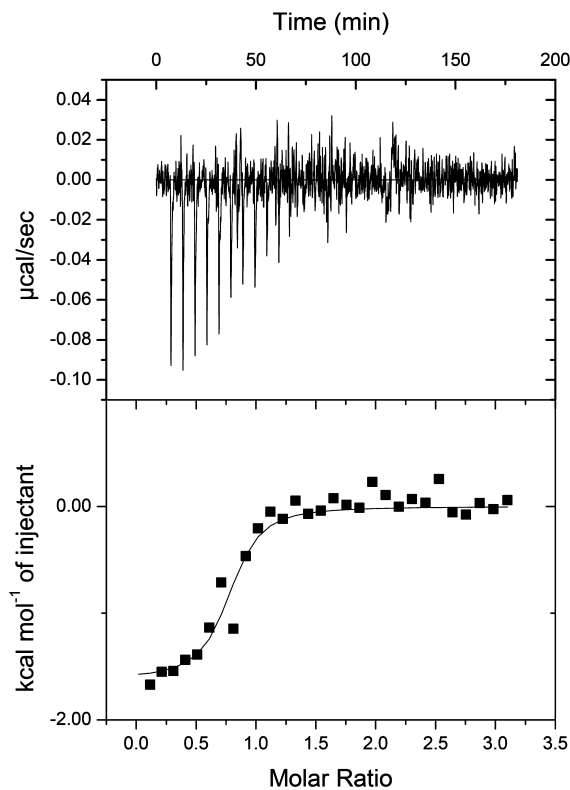


Figure 4. Analysis of the binding of SufE D74R to SufS by isothermal titration calorimetry. SufS in the cell at 50 μ M was titrated with a 10-fold molar excess of SufE D74R. The fitting of the data was derived from the integrated heats of binding plotted against the molar ratio of SufE D74R added to SufS in the cell, after correction for the heat of dilution. The best-fit model was a one binding site model, and the fitted parameters are in Table 1.

only to the absence of the persulfide sulfur on the active site Cys residues of the proteins. The PLP cofactor is present in

SufS_{apo}. The SufS–SufE D74R ITC binding isotherm was exothermic, and the binding data were well-fit using a one-site binding model (Table 1). This result is in direct contrast to SufS–SufE binding data, which best fits a sequential two-site binding model.¹⁰ The results indicate that the binding mode of SufE D74R to SufS is different from that of wild-type SufE. Strikingly, SufE D74R interacts more strongly with SufS than does wild-type SufE. The binding of SufE D74R to SufS showed a $K_d \leq 0.53 \mu$ M, which is 7-fold lower than the first high-affinity binding event of wild-type SufE to SufS under the same conditions ($K_d \leq 3.59 \mu$ M). The number of SufE D74R binding sites on SufS calculated from ITC is only 0.57, indicating that when SufE D74R binds tightly to one SufS monomer the binding of an additional SufE to the other SufS monomer is greatly diminished. This is consistent with negative cooperativity previously found when wild-type SufE_{alk} binds to SufS.¹⁰ Indeed, the binding affinity and binding mode of SufE D74R_{apo} is more similar to results obtained in previous studies using SufE_{alk}, where SufE Cys51 was modified with iodoacetamide (but is otherwise wild-type). Previous HDX-MS and ITC results demonstrated that alkylation of active site Cys51 on SufE increased solvent accessibility and dynamics around Cys51.¹⁰ The increased solvent exposure of alkylated Cys51, which may more closely mimic the sulfur-accepting conformation of the Cys51 loop on wild-type SufE, enhanced the SufE_{alk} binding to SufS. Since the SufE D74R variant behaved similarly to SufE_{alk}, we propose that the D74R substitution changes the environment of Cys51 and shifts its conformation toward the sulfur-accepting state (i.e., more solvent exposed and more dynamic). One prediction of this model is that SufE D74R may be a better substrate for SufS than wild-type SufE during the sulfur mobilization reaction, which could explain the increased enhancement of SufS at high levels of SufE D74R.

SufE D74R Alters SufS Dynamics upon Formation of the SufS–SufE D74R Complex. As stated above, biochemical data are consistent with the D74R substitution affecting the formation of the SufS–SufE complex. In order to better understand the structural differences between the two complexes, HDX-MS was performed on the SufS–SufE D74R complex and results were compared to those determined with SufS alone. Figure 5A shows the perturbations exhibited in SufS upon binding of SufE D74R. Previous studies identified only two peptides in SufS (225–236 and 356–366) that exhibit a decrease in dynamics upon formation of the wild-type SufS–SufE complex.¹⁰ Peptide 225–236 contains Lys226, which forms a Schiff base with the PLP cofactor. Peptide 356–366 contains Cys364, which acts as the sulfur acceptor in the SufS desulfurase reaction. As shown in Figure 5B, deuterium incorporation into these peptides in the SufS–SufE D74R complex is similar to the wild-type complex. In contrast to the wild-type complex, however, there are two additional peptides

Table 1. Fitting Parameters from ITC Analysis of Binding between SufS and Either SufE D74R or SufE_{alk}

SufS + SufE D74R		SufS + SufE _{alk}	
one-site model		one-site model	
Chi ² /DOF	1.672 × 10 ⁴	Chi ² /DOF	2.028 × 10 ⁵
K	1.88 × 10 ⁶ ± 7.16 × 10 ⁵ M ^{−1}	K	(4.06 ± 1.03) × 10 ⁶ M ^{−1}
ΔH	−1757 ± 99.6 cal/mol	ΔH	−8519 ± 123.7 cal/mol
ΔS	22.7 cal/mol/deg	ΔS	1.86 cal/mol/deg
N	0.565 ± 0.0236 sites	N	0.730 ± 0.006 sites

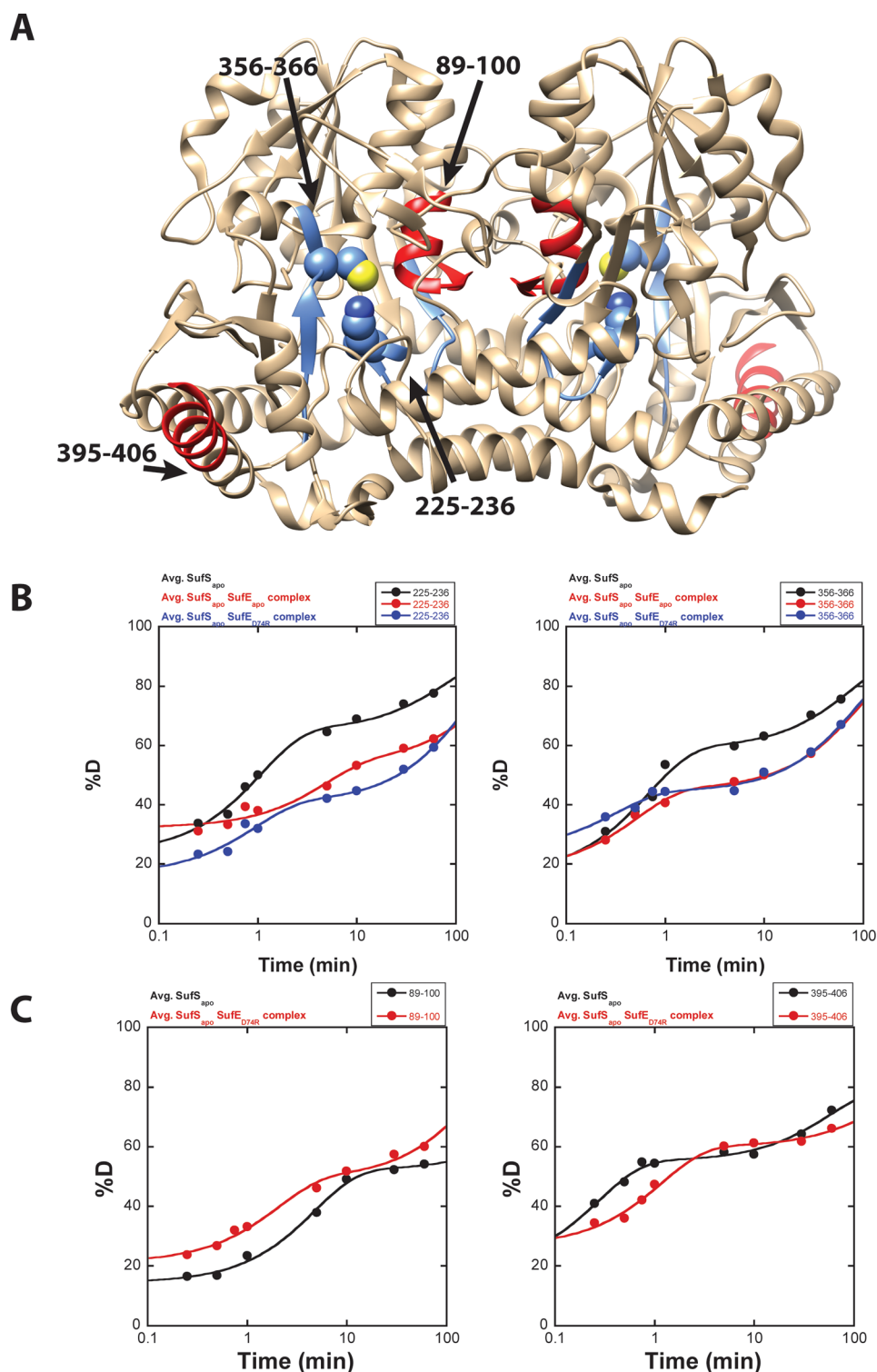


Figure 5. HDX-MS kinetic traces comparing deuterium incorporation as a function of time for SufS and the SufS–SufE D74R complex. (A) SufS peptides exhibiting changes in deuterium exchange parameters upon complex formation with D74R SufE are labeled and highlighted. Key residues in the active site (Lys266 and Cys364) are shown in spheres. (B) Kinetic traces for deuterium incorporation for SufS peptides 225–236 and 356–366 indicate these peptides respond to D74R SufE in a similar fashion when compared to the wild-type complex. (C) Additional differences in deuterium uptake between the wild-type and D74R SufE complexes are seen in peptides 89–100 and 395–406. Fitting parameters can be found in [Supporting Information Table S1](#). The uptake plots for all peptides are found in [Supporting Information Figure S4](#).

of SufS that exhibit changes in deuterium uptake upon formation of the SufS–SufE D74R complex, peptides 89–100 and 395–406 ([Figure 5C](#)). Both regions have overlapping peptides that show similar perturbations upon complex

formation, providing additional support for this set of changes. The region corresponding to peptide 89–100 undergoes an increase in deuterium uptake upon complex formation. This peptide is located at the SufS dimer interface, suggesting that

SufE D74R may influence monomer–monomer communication within the SufS dimer (Figure 5A). Peptide 395–406 is located on a helix involved in the proposed protein–protein interface site and exhibits a decrease in deuterium uptake upon formation of the complex with SufE D74R (Figure 5A). The increase in solvent accessibility is also seen in overlapping peptides in this region. In the native complex, these regions exhibited no change upon SufE binding.

DISCUSSION

Structural Changes of SufE D74R Compared to Wild-Type SufE. SufE Asp74 resides on a small loop, and the main and side chains of Asp74 are predicted to form H-bonds with SufE Gln54 (Figure 6A).¹⁵ These interactions could keep the active site Cys51 loop of SufE locked into a more buried conformation, as seen in resting SufE (Figure 6A). Previous HDX-MS studies indicated that two peptides on wild-type SufE (peptides 38–56 and 66–83) are involved in the interaction with SufS.¹⁰ Peptide 38–56 is a surface loop containing Cys51. Peptide 66–83 forms one side of a structural groove into which the SufE Cys51 thiolate is oriented (Figure 1). Residues within SufE 66–83 may be involved in the SufS interaction, which may cause conformational changes that are propagated to the Cys51 loop. Asp74 is located in peptide 66–83, and Gln54 is located at the Cys51 loop (Figure 6A). HDX-MS analysis of SufE D74R suggests that the D74R substitution induced a conformational change in SufE, making the Cys51 active site loop more dynamic and promoting SufE interaction with SufS. The D74R substitution may prevent Asp74 hydrogen-bond formation with Gln54 due to steric clash, leading to a destabilization of the interaction between the active site loop and the interior groove (Figure 6B). This minor conformational change could promote the exposure of the Cys51 loop and affect the interaction with SufS. Indeed modeling suggests that extension of the SufE active site loop relieves the steric clash caused by the D74R mutation (Figure 6C).

Asp74 Is Not Involved Ionic Interactions between SufE and SufS. On the basis of a putative CsdA–CsdE interaction model derived from the individual structure of CsdE and a homology model structure of CsdA, it was suggested that CsdE Glu84 (or the corresponding Asp74 as conserved in SufE) may provide a charged surface for interactions with cognate cysteine desulfurase enzymes.¹⁵ However, our results indicate that SufE Asp74 is not required for interactions between SufE and SufS. Our findings are consistent with the recently published CsdA–CsdE cocrystal structure, in which the homologous CsdE Glu84 is not directly involved in the interaction with CsdA.¹⁸ Importantly, we found that the interaction between SufE D74R and SufS is 7 times stronger than the interaction between wild-type SufE and SufS. ITC analysis shows that SufE D74R_{apo}–SufS_{apo} binding is more similar to SufE_{alk}–SufS_{apo}, as both are mainly exothermic and best fitted with a one binding site model.¹⁰ However, the number of binding sites (*N*) on SufS calculated from ITC is only 0.57 for SufE D74R_{apo}, which is smaller than the 0.73 sites for SufE_{alk}. It seems that interaction of SufE D74R with one SufS monomer may alter the monomer–monomer interactions within the SufS dimer to reduce the binding of a second SufE to the second SufS monomer. Our hypothesis is that the D74R substitution modulates SufE conformation to mimic the sulfur-accepting state of SufE, which then would likely bind more tightly to SufS.

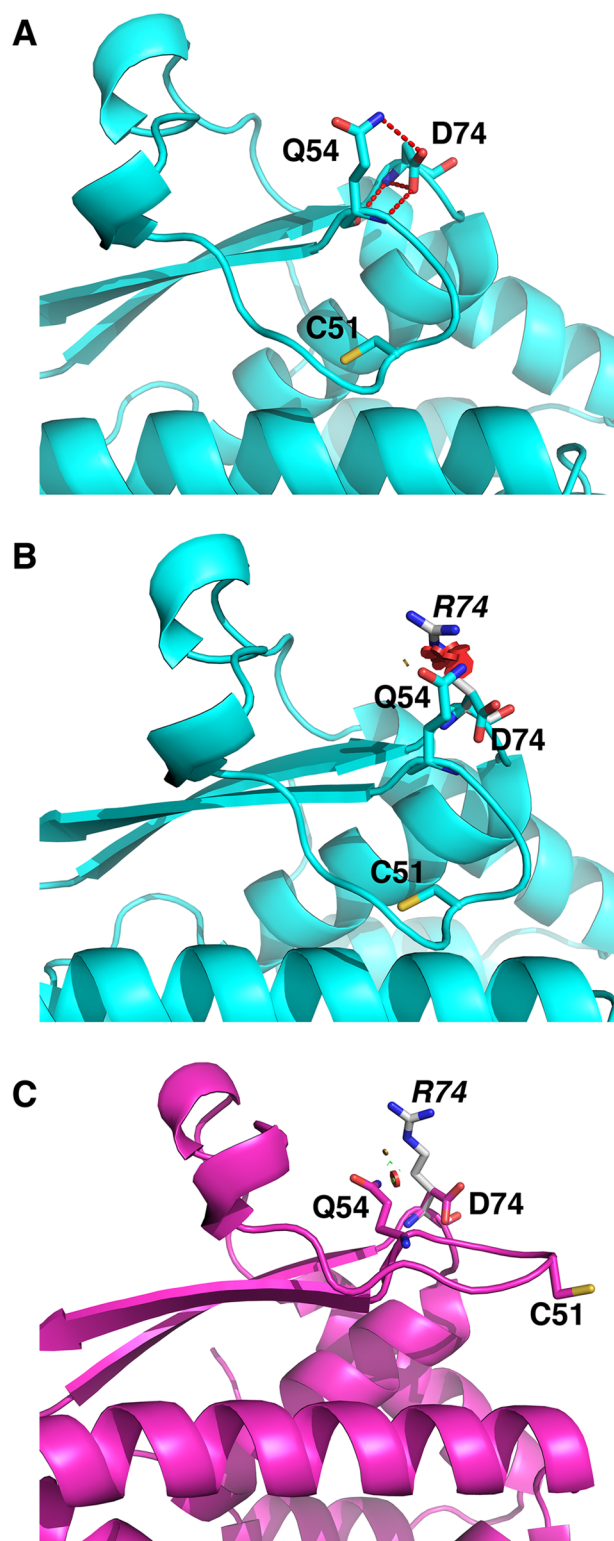


Figure 6. Structural consequences of the SufE D74R mutation. (A) Structure of SufE (PDB 1MZG) showing extensive H-bonding (red dashes) between Q54 and D74 that may stabilize the loop orientation of active site C51. (B) Most likely is that a rotamer of a R74 mutant side chain (gray, italic font label) shows significant van der Waals overlap (red disks) with Q54. (C) Steric clashes (red disks) between R74 (gray, italic font label) and Q54 are alleviated if the C51 loop is in an extended conformation similar to CsdE docked with CsdA (PDB 4LW4). Structural orientation of side chain of D74R point mutant was calculated by PyMOL.

SufE D74R Can Bypass the Saturation Point in the Desulfurase Reaction When Using SufE as a Cosubstrate for SufS. The kinetic analysis of SufS–SufE D74R–L-cysteine reaction indicates that SufS enhancement by SufE D74R does not saturate at the same level as wild-type SufE in the desulfurase reaction (Figure 2A). Formation of the external aldimine between L-cysteine and SufS in the presence of the SufE D74R, monitored via ΔA_{340} , showed sigmoidal behavior. This result is similar to the positive cooperativity of external aldimine formation observed for L-cysteine binding to SufS alone, albeit it is enhanced if SufE D74R is present.¹⁰ The SufE D74R substitution did lower the pK_a of active site Cys51 (Supporting Information Figure S3), which is consistent with a more exposed Cys51 loop conformation. However, the resulting increase in the percentage of deprotonated Cys51 in the mutant protein seems fairly minor, suggesting that the effect on the pK_a of Cys51 was not the main reason for bypassing the saturation point of SufE D74R. The mechanism to explain how this mutant can better enhance SufS activity at higher concentrations is not clear. Possibly, SufE D74R has a faster k_{off} once it receives sulfur from SufS, which becomes more apparent at higher SufE concentrations. This would imply that release of SufE is the rate-limiting step during that portion of the ping-pong reaction. Experiments are underway to examine the detailed kinetics of SufS–SufE interactions and to capture a stabilized SufE D74R–SufS cocomplex for structural analysis.

■ ASSOCIATED CONTENT

■ Supporting Information

Table S1: HDX-MS rate constants and amplitudes for SufE, SufS, and D74R. Table S2: Comparison of different fitting models for kinetic analysis of desulfurase activity assay containing 0.5 μ M SufS, 2 μ M SufE(D74R), and 0–500 μ M L-Cys. Scheme 1: Reaction scheme of SufS, SufE, and L-cysteine. Figure S1: Circular dichroism spectra of wild-type SufE and SufE D74R in the far-UV region and final optical density at 600 nm of MG1655 Δ sufE after 20 h in M9 gluconate minimal media with increasing concentrations of phenazine methosulfate. Figure S2: HDX-MS kinetic profiles for SufE and D74R SufE. Figure S3: Reactions containing 0.5 μ M SufS, SufE_C17S, 2 mM DTT, and 2 mM L-cysteine; pK_a determination of sulfhydryls with PDT-bimane; and activity comparison between SufE and SufE(D74R) at different DTT concentrations. Figure S4: HDX-MS kinetic profiles for SufS and SufS–SufE D74R complex. The Supporting Information is available free of charge on the ACS Publications website at DOI: 10.1021/acs.biochem.5b00663.

■ AUTHOR INFORMATION

Corresponding Authors

*(P.A.F.) Tel.: (205) 348-8349; Fax: (205) 348-9104; E-mail: pfrantom@ua.edu.

*(F.W.O.) Tel.: (803) 777-8151; Fax: (803) 777-9521; E-mail: outtenf@mailbox.sc.edu.

Present Address

§(Y.D.) Department of Surgery, School of Medicine, University of California, San Francisco, California 94109, United States.

Funding

This work was supported by NSF grant MCB 0845273 (L.S.B.) and NIH grants GM 81706 (F.W.O.) and GM 112919 (F.W.O. and P.A.F.). The UA Mass Spectrometry facility is supported by CRIF grant CHE 0639003.

Notes

The authors declare no competing financial interest.

■ ACKNOWLEDGMENTS

The authors would like to acknowledge Maks Chruszcz for many insightful suggestions.

■ DEDICATION

This study is dedicated to the memory of Laura Busenlehner, a wonderful colleague and friend who was taken from us too soon.

■ ABBREVIATIONS

HDX-MS, hydrogen–deuterium exchange mass spectrometry; Fe–S, iron–sulfur; PLP, pyridoxal 5'-phosphate

■ REFERENCES

- (1) Loiseau, L., Ollagnier-de-Choudens, S., Nachin, L., Fontecave, M., and Barras, F. (2003) Biogenesis of Fe-S cluster by the bacterial Suf system: SufS and SufE form a new type of cysteine desulfurase. *J. Biol. Chem.* 278, 38352–38359.
- (2) Outten, F. W., Wood, M. J., Munoz, F. M., and Storz, G. (2003) The SufE protein and the SufBCD complex enhance SufS cysteine desulfurase activity as part of a sulfur transfer pathway for Fe-S cluster assembly in *Escherichia coli*. *J. Biol. Chem.* 278, 45713–45719.
- (3) Layer, G., Gaddam, S. A., Ayala-Castro, C. N., Ollagnier-de-Choudens, S., Lascoux, D., Fontecave, M., and Outten, F. W. (2007) SufE transfers sulfur from SufS to SufB for iron-sulfur cluster assembly. *J. Biol. Chem.* 282, 13342–13350.
- (4) Mihara, H., Maeda, M., Fujii, T., Kurihara, T., Hata, Y., and Esaki, N. (1999) A nifS-like gene, csdB, encodes an *Escherichia coli* counterpart of mammalian selenocysteine lyase. Gene cloning, purification, characterization and preliminary x-ray crystallographic studies. *J. Biol. Chem.* 274, 14768–14772.
- (5) Fujii, T., Maeda, M., Mihara, H., Kurihara, T., Esaki, N., and Hata, Y. (2000) Structure of a NifS homologue: X-ray structure analysis of CsdB, an *Escherichia coli* counterpart of mammalian selenocysteine lyase. *Biochemistry* 39, 1263–1273.
- (6) Mihara, H., Kurihara, T., Yoshimura, T., and Esaki, N. (2000) Kinetic and mutational studies of three NifS homologs from *Escherichia coli*: mechanistic difference between L-cysteine desulfurase and L-selenocysteine lyase reactions. *J. Biochem.* 127, 559–567.
- (7) Lima, C. D. (2002) Analysis of the *E. coli* NifS CsdB protein at 2.0 Å reveals the structural basis for perselenide and persulfide intermediate formation. *J. Mol. Biol.* 315, 1199–1208.
- (8) Dai, Y., and Outten, F. W. (2012) The *E. coli* SufS–SufE sulfur transfer system is more resistant to oxidative stress than IscS–IscU. *FEBS Lett.* 586, 4016–4022.
- (9) Selbach, B. P., Pradhan, P. K., and Dos Santos, P. C. (2013) Protected sulfur transfer reactions by the *Escherichia coli* Suf system. *Biochemistry* 52, 4089–4096.
- (10) Singh, H., Dai, Y., Outten, F. W., and Busenlehner, L. S. (2013) *Escherichia coli* SufE sulfur transfer protein modulates the SufS cysteine desulfurase through allosteric conformational dynamics. *J. Biol. Chem.* 288, 36189–36200.
- (11) Mihara, H., Fujii, T., Kato, S., Kurihara, T., Hata, Y., and Esaki, N. (2002) Structure of external aldimine of *Escherichia coli* CsdB, an IscS/NifS homolog: implications for its specificity toward selenocysteine. *J. Biochem.* 131, 679–685.
- (12) Urbina, H. D., Cupp-Vickery, J. R., and Vickery, L. E. (2002) Preliminary crystallographic analysis of the cysteine desulfurase IscS from *Escherichia coli*. *Acta Crystallogr., Sect. D: Biol. Crystallogr.* 58, 1224–1225.
- (13) Cupp-Vickery, J. R., Urbina, H., and Vickery, L. E. (2003) Crystal structure of IscS, a cysteine desulfurase from *Escherichia coli*. *J. Mol. Biol.* 330, 1049–1059.

- (14) Shi, R., Proteau, A., Villarroya, M., Moukadiri, I., Zhang, L., Trempe, J. F., Matte, A., Armengod, M. E., and Cygler, M. (2010) Structural basis for Fe-S cluster assembly and tRNA thiolation mediated by IscS protein-protein interactions. *PLoS Biol.* 8, e1000354.
- (15) Goldsmith-Fischman, S., Kuzin, A., Edstrom, W. C., Benach, J., Shastry, R., Xiao, R., Acton, T. B., Honig, B., Montelione, G. T., and Hunt, J. F. (2004) The SufE sulfur-acceptor protein contains a conserved core structure that mediates interdomain interactions in a variety of redox protein complexes. *J. Mol. Biol.* 344, 549–565.
- (16) Liu, G., Li, Z., Chiang, Y., Acton, T., Montelione, G. T., Murray, D., and Szyperski, T. (2005) High-quality homology models derived from NMR and X-ray structures of *E. coli* proteins YgdK and SufE suggest that all members of the YgdK/SufE protein family are enhancers of cysteine desulfurases. *Protein Sci.* 14, 1597–1608.
- (17) Guzzo, C. R., Silva, L. R., Galvao-Botton, L. M., Barbosa, J. A., and Farah, C. S. (2006) Expression, crystallization and preliminary crystallographic analysis of SufE (XAC2355) from *Xanthomonas axonopodis* pv. citri. *Acta Crystallogr., Sect. F: Struct. Biol. Cryst. Commun.* 62, 268–270.
- (18) Kim, S., and Park, S. (2013) Structural changes during cysteine desulfurase CsdA and sulfur acceptor CsdE interactions provide insight into the trans-persulfuration. *J. Biol. Chem.* 288, 27172–27180.
- (19) Busenlehner, L. S., and Armstrong, R. N. (2005) Insights into enzyme structure and dynamics elucidated by amide H/D exchange mass spectrometry. *Arch. Biochem. Biophys.* 433, 34–46.
- (20) Bolstad, H. M., and Wood, M. J. (2010) An in vivo method for characterization of protein interactions within sulfur trafficking systems of *E. coli*. *J. Proteome Res.* 9, 6740–6751.